



Study on condensation heat transfer characteristics of wet paper in steam heating process

Tsutomu Kawamizu^{a,*}, Takeshi Kaneko^b, Setsuo Suzuki^c, Takaharu Tsuruta^d

^aHiroshima Research & Development Center, Mitsubishi Heavy Industries, Ltd., 6-22, 4-chome, Kan-on-shin-machi, Nishi-ku, Hiroshima 733-8553, Japan

^bHiroshima Research & Development Center, Mitsubishi Heavy Industries, Ltd., 1-1, Itozaki minami 1-chome, Mihara, Hiroshima 729-3939, Japan

^cPaper & Printing Machinery Division, Mitsubishi Heavy Industries, Ltd., 1-1, Itozaki minami 1-chome, Mihara, Hiroshima 729-3939, Japan

^dDepartment of Mechanical Engineering, Kyushu Institute of Technology, 1-1, Sensui, Tobata-ku, Kitakyushu 804-8550, Japan

ARTICLE INFO

Article history:

Received 9 November 2007

Received in revised form 9 July 2008

Available online 29 September 2008

Keywords:

Porous media

Permeability

Suction pressure

Condensation

Heat transfer

Mass transfer

ABSTRACT

Effects of suction pressure and permeability on the steam heating characteristics of the wet paper are studied. Experimental results show that suction pressure enhances the energy absorption in the wet paper and effects of suction pressure strongly appear in the high-permeability paper, and also absorbed energy rate is decreased with increasing in heating time. From the numerical simulation results it is found that increase in moisture content and decrease of pressure gradient reduce the absorbed energy rate. Dimensionless numbers are derived from the basic equations to summarize the experimental and numerical simulation results.

© 2008 Elsevier Ltd. All rights reserved.

1. Introduction

The paper manufacture industry is continuing development of new procedures for removing more water before drying in the press section of the paper making machine. Hot pressing is a technique to enhance the water removal by heating the wet paper in the press section. It is well known that 10 °C rise in the ingoing wet paper temperature decreases outgoing moisture content by 1% [1]. This is due to decrease of water viscosity and surface tension by increasing the temperature. Steam is one convenient source to heat the wet paper for the paper making machine and a steam box has been used for the hot pressing. Often times, the steam box is used in conjunction with a suction box, because the suction box causes a pressure-driven flow through the wet paper and pulls the steam into the wet paper. Thus the suction box improves the ability to heating the wet paper. From the technical point of view, effects of the suction box on the steam heating characteristics are mostly estimated by the pilot or mill trial results, but key factors in the steam heating of the wet paper have not been well identified [2]. Patterson et al. pointed out the effectiveness of this technique and made a series of experimental investigations using a unique experimental apparatus [3–5]. Their experimental results show that steam penetration and heating characteristics

in the wet paper are primarily governed by the permeability of the wet paper. But details of heat and mass transfer in the wet paper, such as absorbed energy rate, moisture contents and pressure distributions have not been studied clearly.

In this paper, we study experimentally and analytically the effects of suction pressure on the steam heating characteristics in the wet paper. Temperature distribution and absorbed energy are estimated by the experimental measurements. Time transients of the moisture and pressure distributions in the paper-thickness direction are studied numerically. Dimensionless numbers are derived from the basic equations, which are relating to the steam flow rate and the energy absorption rate. We apply these dimensionless numbers to summarize the experimental and numerical simulation results.

2. Experimental apparatus and method

The experimental apparatus used in this investigation is shown in Fig. 1. The test sample of wet paper is clamped on a suction box and the pressure of suction box is reduced by a vacuum pump. There is a large volumetric buffer tank between the suction box and the vacuum pump, which prevents fluctuation of the suction pressure during the experiment. The steam box equipped with the metallic mesh for a uniform steam flow into the test sample is mounted on the linear guide, and it can move at 500 mm/s using this linear guide. Steam generated in the boiler is supplied to the

* Corresponding author. Tel.: +81 82 294 9827; fax: +81 82 294 9179.
E-mail address: tsutomu_kawamizu@mhi.co.jp (T. Kawamizu).

Nomenclature

a_p	Thermal diffusivity of paper ($=\lambda_p/(\rho_p C_{pp})$) [m^2/s]	x	Distance from top surface [m]
C_p	Specific heat [J/(kg K)]	Z	Moisture content (Dry basis) [-]
D	Capillary conductivity [m^2/s]	<i>Greek symbols</i>	
Da	Darcy number [-]	ε	Porosity [-]
h_{fg}	Latent heat of condensation [J/kg]	ρ	Density [kg/m^3]
k	Permeability [m^2]	λ_p	Thermal conductivity of wet paper [W/(m K)]
k_{fs}	Permeability at the fiber saturation point [m^2]	μ	Viscosity [Pa s]
k_{rv}	Relative permeability (gas) [-]	ν	Kinetic viscosity [m^2/s]
L	Characteristic length scale ($=t_p$) [m]	ϕ	Moisture content (Wet basis) [-]
\dot{m}	Mass flux [$kg/(m^2 s)$]	π_1	Dimensionless suction pressure [-]
\dot{m}_c	Steam condensation rate [$kg/(m^3 s)$]	π_2	Dimensionless absorbed energy rate [-]
m	Mass per unit area [kg/m^2]	π'_2	Dimensionless average absorbed energy rate (80% heat input) [-]
nl	Number of layer [-]	θ	Dimensionless temperature [-]
P	Pressure [Pa]	Ω	Dimensionless mass flow rate of steam ($=Da\pi_1$) [-]
P^*	Dimensionless pressure [-]	<i>Subscripts/superscripts</i>	
Ph'	Modified phase change number [-]	0	Reference value
Pr'	Modified Prandtl number [-]	at	Atmosphere
ΔP	Pressure difference [Pa]	c	Capillary
Q	Absorbed energy [J/ m^2]	d	Bulk
\bar{Q}	Average absorbed energy rate [W/ m^2]	f	Fiber (=Bone dry paper)
\bar{Q}	Average absorbed energy rate (80% heat input) [W/ m^2]	fs	Fiber saturation point
\dot{Q}^t	Absorbed energy rate [W/ m^2]	g	Gas
s	Water saturation [-]	i	Initial value
Sc'	Modified Schmidt number [-]	l	Water
T	Temperature [$^{\circ}C$]	n	Empirical factor
t	Time [s]	p	Paper
t^*	Dimensionless time [-]	sat	Saturation
t_p	Paper thickness [m]	suc	Suction
u	Darcy velocity [m/s]	t	Time
U	Dimensionless velocity [-]	v	Steam
X	Dimensionless length [-]		

steam box through the steam tube. The steam tube is heated by the electrical heater to prevent condensation not only in the steam tube but also in the steam box; that is, the steam is slightly super heated at 103 or 110 $^{\circ}C$. The mass flow rate of steam is 9 kg/h, which is enough for the steam heating experiments.

To evaluate the effects of permeability and thickness on the steam heating characteristics, the handsheets of a newsprint and a fine paper with the basis weight (weight of bone dry paper/paper area) of 100 g/ m^2 and 200 g/ m^2 are used in the experiments. As described later, the permeability of the newsprint and fine paper are greatly different, and the thickness of the wet paper changes in proportion to the basis weight. The test samples are multi-ply pa-

pers having a thermocouple embedded between each layer as shown in Fig. 2. Both surface temperatures are also measured with thermocouples. The thermocouples used in all experiments are the Type K bare-wire thermocouples with 0.025 mm diameter. The test sample is pressed at 1.37 MPa for 5 min, so thermocouples and wet paper are bounded tightly. The shape of the test sample is a square 125 mm on a side. Fig. 2 shows details of the test section placed on the top of the suction box. A coordinate x is set from the top surface of the test sample which thickness is denoted by t_p . The top of the suction box is made of teflon and has an opening area of 50 mm square for the suction flow. To prevent the deformation of the test sample in the suction area, a wire mesh and a felt sheet are used to

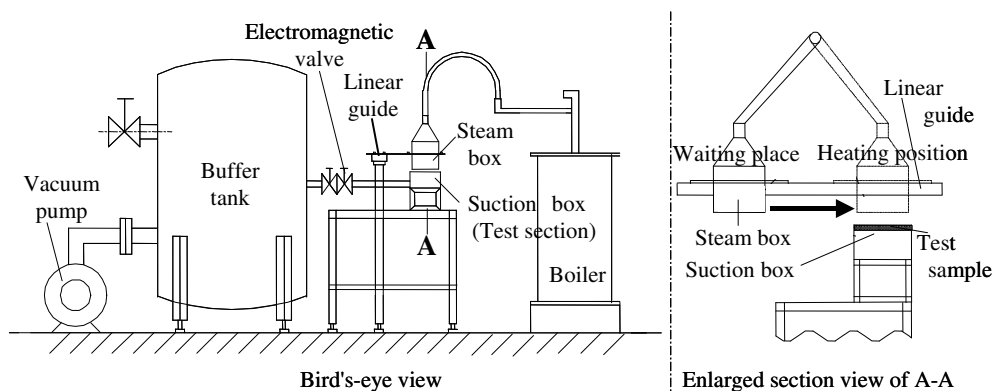


Fig. 1. Schematic of experimental apparatus.

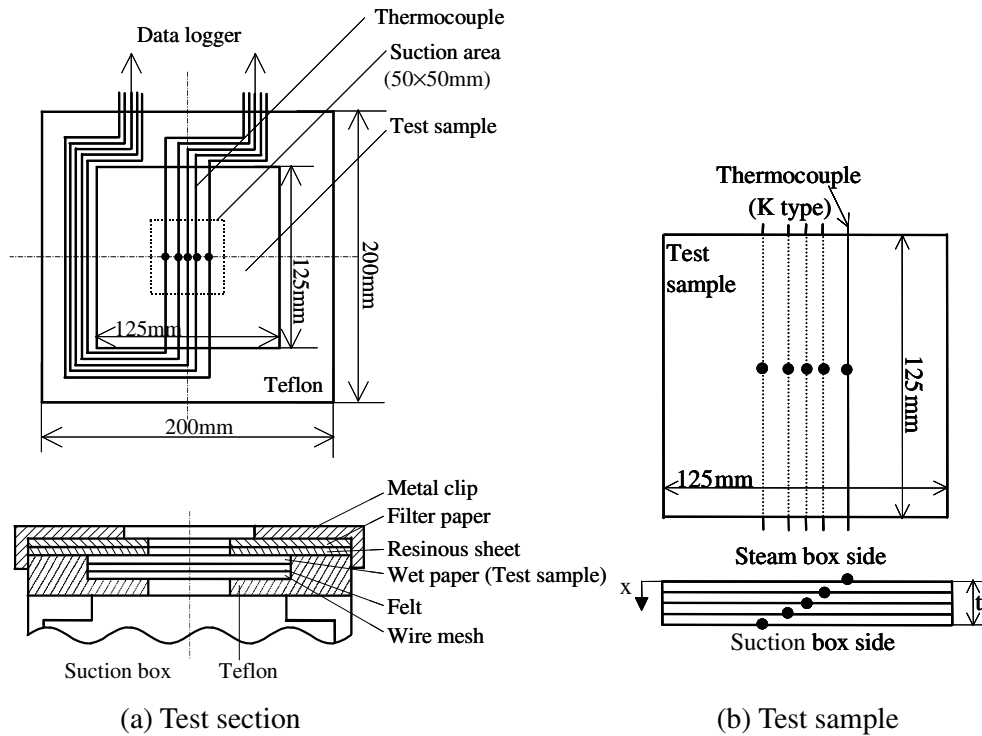


Fig. 2. Details of test section and test sample.

support the wet paper. The permeability of the wire mesh and felt are much larger than that of the wet paper. So, the steam flow rate through the wet paper is dominated by the permeability of the wet paper. A filter paper and resinous sheet are located between the top surface of wet paper and metal clip. A resinous sheet restrains aspiration of the air and steam from the outside of the suction area. The filter paper prevents droplet absorption into the wet paper; because the droplet is generated by the condensation at a metal clip.

The moisture content of the test sample may change during the installation of the test sample on the experimental device and the waiting period for the pre-steady state. The pre-steady state means that the suction flow is introduced but steam is not supply to the test sample. To get the desired initial moisture content in the steam heating experiment, we use a calibration curve which takes into account the evaporation before the test. After the moisture content of the test sample and steam temperature come to be the targeted values, the pressure of the buffer tank is reduced to the desired value by the vacuum pump. Then an electromagnetic valve is opened to allow the suction to be applied the test sample; the steam box moves from a waiting place to the heating position after the pressure of the suction box and the pressure distribution in the test sample reach steady state.

The experimental conditions and characteristics of paper are respectively shown in Tables 1 and 2. The moisture content ϕ is a wet basis moisture content (weight of water/(weight of water +

Table 1
Experimental conditions

Grade	Basis weight [g/m ²]	Number of thermocouples	Initial moisture content ϕ_i [-]	Suction pressure (Gauge)[kPa]
Newsprint	100	5	0.55	0, -25, -46
Fine paper	100	5	0.55	0, -5, -15, -25
	200	5	0.55	0, -5, -15, -25

Table 2
Characteristics of paper

Grade	Newsprint	Fine paper
Basis weight [g/m ²]	100	100, 200
Paper thickness t_p [μ m], $\phi = 0.55$ [-]	300 (100[g/m ²])	280 (100 [g/m ²]) 560 (200 [g/m ²])
Fiber saturation point ϕ_{fs} [-]	0.383	0.438
Porosity ε [-], $\phi = \phi_{fs}$ [-]	0.572	0.483
Permeability k [m ²], $\phi = 0.55$ [-]	8.43×10^{-15}	1.02×10^{-13}
Permeability k_{fs} [m ²], $\phi = \phi_{fs}$ [-]	2.66×10^{-14}	1.55×10^{-13}
Relative permeability k_{rv} [-]	$(1-s)^3$	$(1-s)^2$
Capillary conductivity D [m ² /s]	Han $\times 0.25$, 1.0	Han $\times 1.0$, 4.0
Density (Bulk) [kg/m ³], $\phi = 0.55$ [-]	740	793
Specific heat (Bulk) [J/(kg K)], $\phi = 0.55$ [-]	2893	2893
Thermal conductivity (Bulk) [W/(m K)], $\phi = 0.55$ [-]	0.456	0.456

weight of bone dry paper)). Thermal conductivity of the wet paper is obtained by a regression formula, which considers the effect of moisture content [6,7]. The permeability of paper is estimated by the Darcy's law.

$$k = \frac{\mu_g u t_p}{\Delta P} \tag{1}$$

where k is the permeability, u is the Darcy velocity.

The volumetric flow rate and Darcy velocity are evaluated by the results of Gurley method (JIS (Japanese Industrial Standards) P 8117). The thickness of paper is tested in accordance with JIS P 8118. The relation between moisture content and permeability of wet paper is shown in the Fig. 3. The thickness of wet paper with a basis weight of 50 g/m² is shown in Fig. 4. The permeability and thickness of paper have an inflection point. The wet paper consists of liquid (water) and gas (air etc) in a matrix of porous solid (fiber). It is considered that this inflection point is related to the fiber saturation point [8]. At moisture contents less than the fiber saturation point; the water is contained in only the intra-fiber

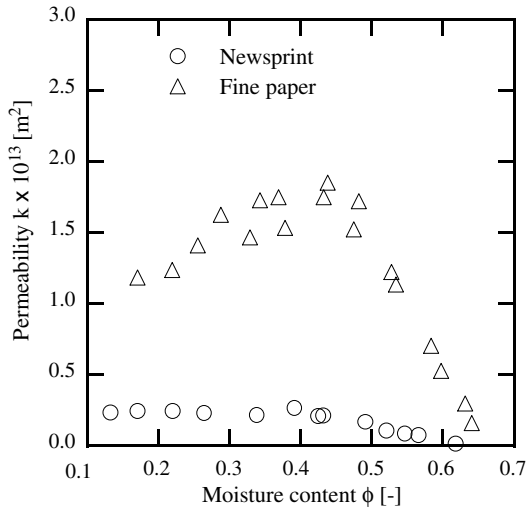


Fig. 3. Permeability of paper.

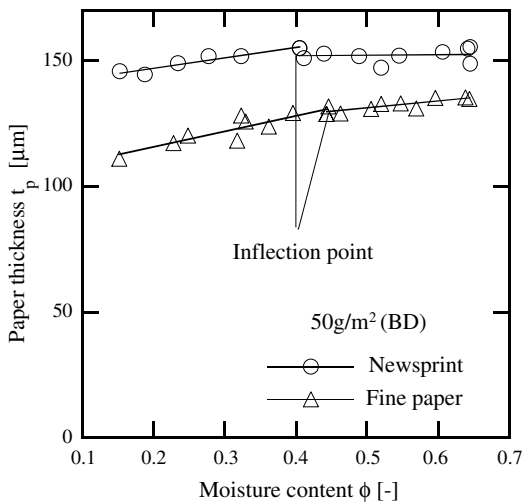


Fig. 4. Paper thickness (50 g/m²).

pores and water saturation can be treated as 0. Here, water saturation denotes the fraction of pore space occupied by the inter-fiber water. So the thickness of wet paper increases with the moisture content. At higher moisture contents than the fiber saturation point, the water is contained in the inter-fiber pore and the permeability of the wet paper decreases with increasing moisture content. Hence, water saturation is increased with moisture content. From the Table 2, Figs. 3 and 4, we can understand that the permeability of the newsprint is much smaller than that of fine paper at the initial moisture content of 0.55 while the difference of thickness is small. Also, the fiber saturation point corresponds to the inflection point shown in Figs. 3 and 4.

3. Experimental results

The absorbed energy is calculated by the following equations using the measured temperature. Fig. 5 shows one layer of the test sample, the average temperature of one layer is evaluated by

$$\bar{T}_i^t = (T_i^t + T_{i+1}^t)/2. \quad (2)$$

Where T_i^t and T_{i+1}^t denote the measured temperatures of the upper and lower surfaces of the layer i at the time t , respectively. Absorbed

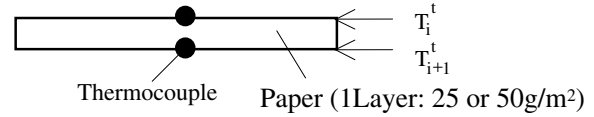


Fig. 5. Calculation method of absorbed energy.

energy Q_i^t of the layer i within each sampling time Δt is estimated by Eq. (3). In this experiment, data sampling rate is 200 Hz and Δt is 5 ms.

$$Q_i^t = (C_{pl}m_i + C_{pf}m_f)(\bar{T}_i^{t+\Delta t} - \bar{T}_i^t) \quad (3)$$

Where C_{pl} and C_{pf} are the specific heat of the water and fiber. m_i , m_f denote the mass per unit area of water and fiber (=bone dry paper) in layer i . Absorbed energy Q^t of the test sample within each sampling time is calculated by summing the absorbed energy of each layer. Absorbed energy rate \dot{Q}^t is calculated by Eq. (5).

$$Q^t = \int_{x=0}^{t_p} Q_x^t dx = \sum_{i=1}^{nl} Q_i^t \quad (4)$$

$$\dot{Q}^t = \int_{x=0}^{t_p} Q_x^t dx / \Delta t = Q^t / \Delta t \quad (5)$$

Where nl is the number of layers. Absorbed energy Q of the test sample within steam heating period t is evaluated by Eq. (6), and average absorbed energy rate is calculated by Eq. (7).

$$Q = \int_0^t Q^t dt = \sum_{t=0}^t Q^t \quad (6)$$

$$\dot{Q} = Q/t \quad (7)$$

Fig. 6 shows temperature distribution and absorbed energy rate \dot{Q}^t for the newsprint and fine paper with a basis weight of 100 g/m² at the suction pressures 0 and –25 kPa. When the suction pressure is 0 kPa, the pressure in the suction box is equal to the atmospheric pressure. Then the suction box does not cause the pressure-driven flow and there is no suction effect on the steam heating of the wet paper. In this case, $\Delta P = 0$ kPa, the newsprint (Fig. 6 (a)) and fine paper (Fig. 6 (c)) have a similar temperature distribution and absorbed energy rate, and the large temperature difference occurs along the thickness direction during the steam heating period. Here, a definition of ΔP is a pressure difference between the atmosphere and the suction box. It is considered that paper grade does not affect the steam heating characteristics and heat conduction dominates the heat transfer in the wet paper. In the case of $\Delta P = 25$ kPa, the absorbed energy rate is increased and the temperature difference at $t = 0.1$ s is reduced because the bottom surface ($x/t_p = 1.0$) temperature rises quickly. Temperature at the $x/t_p = 0.25$ almost becomes the steady state temperature before initiating the temperature rise at the bottom surface ($x/t_p = 1.0$). This means that the steam raises the temperature of each position to the equilibrium temperature and the condensation region extends from the top to the bottom surface. For the fine paper at $\Delta P = 25$ kPa, the steady state temperature at each location gets to the equilibrium temperature. That is, in Fig. 6(d), the temperature of the bottom surface ($x/t_p = 1.0$) at $t = 0.5$ s is almost same as 92.2 °C, which is the equilibrium temperature for the suction pressure –25 kPa. The absorbed energy rate has a maximum value immediately after the initiation of steam heating, and the absorbed energy rate is decreased with increasing in the steam heating time. It is considered that increasing of moisture content at the surface region reduces the permeability of wet paper and the spreading of the condensation region decreases the pressure gradient, which reduce the mass flow rate of steam into the wet paper and absorbed energy rate. From Fig. 6(b) and (d), we can see that effects of the suction pressure strongly appear in

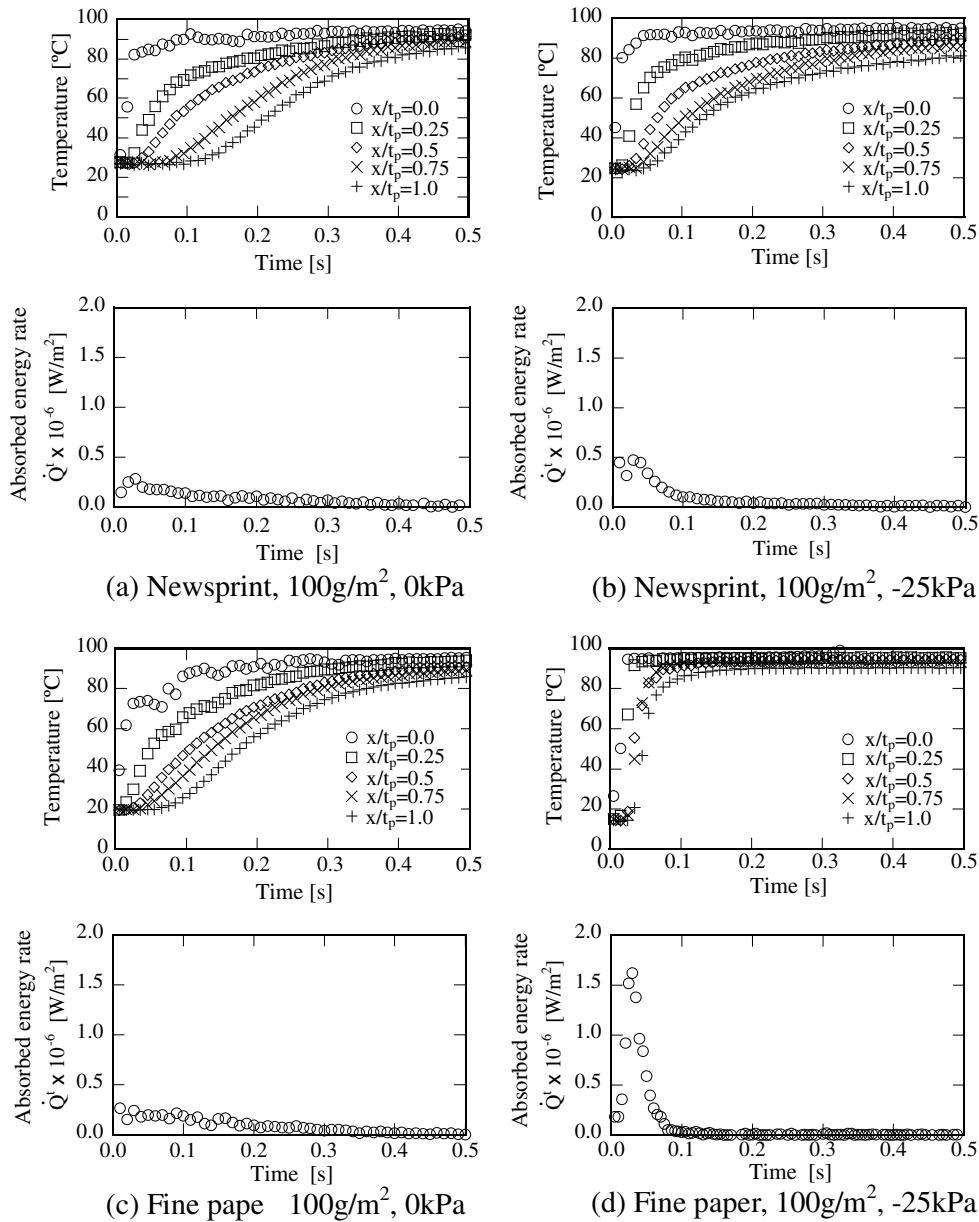


Fig. 6. Temperature distribution and absorbed energy rate (100 g/m²).

the fine paper. Maximum absorbed energy rate of the fine paper is almost three times larger than that of the newspaper. This is because as shown in Table 2 and Fig. 3, the fine paper has a higher permeability than the newspaper. At the initial moisture content point, the permeability of the fine paper is about ten times that of the newspaper. Furthermore, from Fig.6(b), in the case of newspaper, it seems that internal steam condensation heats only near the surface region, and the heating due to the internal steam condensation disappears immediately and heat conduction dominates the heat transfer in the wet paper. On the other hand, for the fine paper (Fig. 6(d)), it seems that most of the region is directly heated by the internal steam condensation.

The relation between the suction pressure and the absorbed energy at $t = 30, 50, 100$ ms is shown in Fig. 7. As mentioned above the suction pressure enhances the energy absorption in the wet paper, and effects of the suction pressure strongly appear in the fine paper. For the newspaper, at $t = 30, 50$ ms, even in the large suction pressure such as -46 kPa, the absorbed energy is almost equal to that for the fine paper at the suction pressure -5 kPa. Since the

permeability of the newspaper is about one-tenth of the fine paper, it is interesting to note that we have almost same the steam flow rates and absorbed energies when the suction pressure for the newspaper is about ten-times larger than the fine paper. But at $t = 100$ ms, the newspaper has a smaller absorbed energy than the fine paper. The condensation heat transfer depends on the suction flow of steam characterized by the permeability as well as the water mobility due to the capillarity. Details of these effects will be discussed in Section 5.

4. Analysis

4.1. Numerical simulation model

A one-dimensional numerical simulation model has been developed. The followings are the mass, momentum and energy conservation equations used by the model; details of this model are described in the previous work [9].

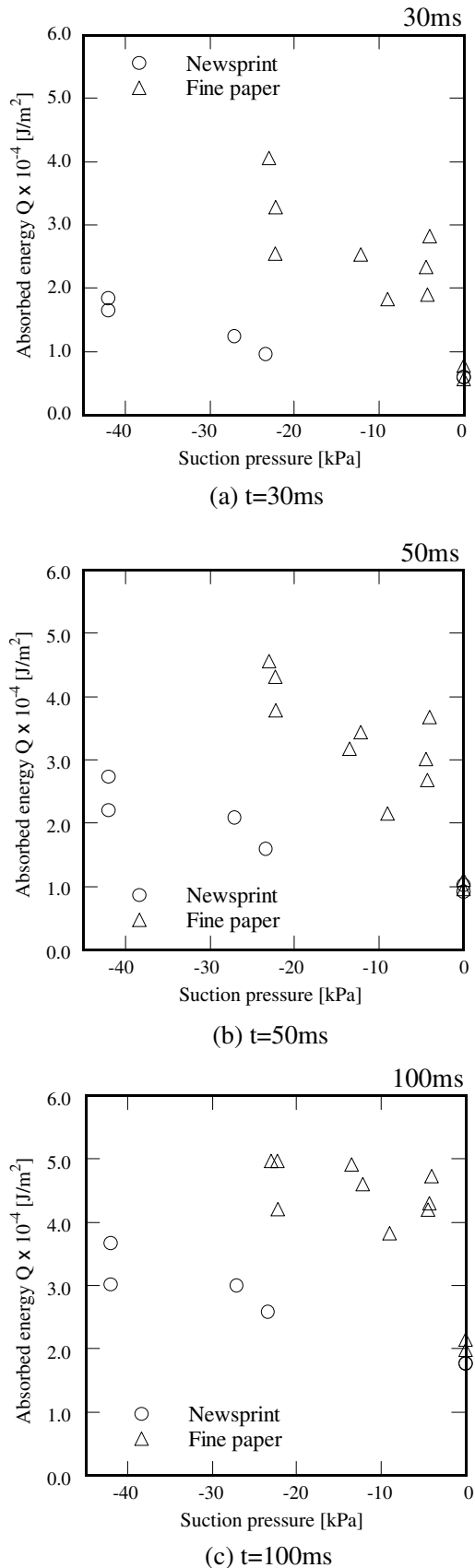


Fig. 7. Absorbed energy (100 g/m²).

4.1.1. Mass conservation

Mass conservation equations for steam and water are expressed by Eqs. (8) and (9).

$$\text{(Steam)} \quad \frac{\partial}{\partial x} (\rho_v u_v) + \dot{m}_c = 0 \quad (8)$$

$$\text{(Water)} \quad \varepsilon \frac{\partial}{\partial t} (\rho_1 s) = -\frac{\partial}{\partial x} (\rho_1 u_1) + \dot{m}_c \quad (9)$$

where \dot{m}_c is steam condensation rate in the wet paper, ε is the porosity, and s is the water saturation denoting the fraction of pore space occupied by the inter-fiber water.

4.1.2. Momentum conservation

Momentum conservation equations for steam and water are respectively written by

$$\text{(Steam)} \quad \dot{m}_v = -\rho_v \frac{k_{rv} k_{fs}}{\mu_v} \frac{\partial P_v}{\partial x} \quad (10)$$

$$\text{(Water)} \quad \dot{m}_1 = \rho_1 \frac{k_1}{\mu_1} \frac{\partial P_c}{\partial x} = -\rho_d D \frac{\partial Z}{\partial x} \quad (11)$$

where k_{fs} denotes the permeability of the wet paper at the fiber saturation point, k_{rv} is the relative permeability for gas. k_1 is the permeability for the water, and D is the capillary conductivity. ρ_d , P_c and Z denote the bulk density of the fiber, capillary pressure and moisture content (dry basis), respectively.

The relative permeability can be given by the empirical formula [10].

$$k_{rv} = (1 - s)^n \quad (12)$$

Here n is the empirical factor estimated by the experimental data. This empirical factor n is evaluated by using relation between water saturation (moisture content) and permeability that we measured (Fig. 3). From the comparison with measured results, we find that the relative permeability is appropriately expressed when we use a value of $n = 2$ for the fine paper and $n = 3$ for the newsprint. It is considered that the paper structure and material composition make difference to the mass transfer characteristics in the paper.

In porous media, such as paper, the capillary pressure for water flow is proportional to the moisture content. In order to express the capillary flow rate, a capillary conductivity D is derived [11,12]. We are using the capillary conductivity D based on the experimental result by Han and Ulmanen that is the average value in the literature [11], but it depends on the paper structure, material composition, etc. Therefore the parametric calculation for the capillary conductivity is carried out.

4.1.3. Energy conservation

The energy conservation equation in the wet paper can be simplified as follow.

$$\varepsilon \frac{\partial}{\partial t} (s \rho_1 C_{pl} T + \frac{1 - \varepsilon}{\varepsilon} \rho_{fs} C_{pfs} T) = -\frac{\partial}{\partial x} (\rho_v u_v h_{fg}) + \frac{\partial}{\partial x} (\lambda_p \frac{\partial T}{\partial x}) \quad (13)$$

Thermal conductivity of the wet paper is obtained by a regression formula, which considers the effect of moisture content [6,7].

$$\lambda_p = 0.34 \frac{\phi}{1 - \phi} + 0.040 \quad (14)$$

The specific heat and density of the saturated fiber in Eq. (13) are expressed in the following equations.

$$C_{pfs} = \phi_{fs} C_{pl} + (1 - \phi_{fs}) C_{pf} \quad (15)$$

$$\rho_{fs} = \frac{1}{(1 - \varepsilon)(1 - \phi_{fs})} \rho_d \quad (16)$$

$C_{pf} = 1.3 \times 10^3$ [J/(kg K)] is the specific heat of the fiber. Properties of the wet paper are shown in the Table 2.

Temperature, moisture (water saturation) and pressure distributions in the thickness direction are obtained with the finite difference method. Basic conservation equations, Eqs. (8)–(11) and (13), are numerically solved by the explicit method [13]. The steam

flow rate is calculated by equating the pressure drop in the wet paper to the suction pressure difference, and condensation rate is set as same as this mass flow rate until the temperature of wet paper becomes steady state.

4.2. Dimensionless number

Using following characteristics values and dimensionless quantities, we derive the dimensionless numbers from the basic equations that denote the feature of steam heating of the wet paper.

4.2.1. Characteristics value

Length $L = t_p$ (17)

Velocity $u_0 = \frac{k_i}{\mu_v} \frac{\Delta P}{t_p}$ (18)

Time $t_0 = L/u_0$ (19)

Temperature $\Delta T = T_{sat} - T_i$ (20)

Pressure $\Delta P = P_{at} - P_{suc}$ (21)

Where t_p is the paper thickness. k_i is permeability of the wet paper at the initial moisture content. T_{sat} and T_i denote the saturated temperature and initial temperature of the wet paper, respectively. P_{at} and P_{suc} are the atmospheric and suction pressure.

4.2.2. Dimensionless quantity

Length $X = x/L$ (22)

Velocity $U = u/u_0$ (23)

Time $t^* = \frac{u_0 t}{L} = \frac{k_i}{\mu_v} \frac{\Delta P}{t_p^2} t$ (24)

Temperature $\theta = (T - T_i)/\Delta T$ (25)

Pressure $P^* = (P - P_{suc})/\Delta P$ (26)

4.2.3. Dimensionless number

Modified Prandtl number $Pr' = \nu_v/a_p$ (27)

Modified Schmidt number $Sc' = \nu_v/D$ (28)

Modified phase change number (= Jakob number) (29)

$Ph' = (C_{pp}\Delta T)/h_{fg}$

Darcy number $Da = k_i/L^2$ (30)

Dimensionless suction pressure $\pi_1 = \frac{\rho_v L^2 \Delta P}{\mu_v^2}$ (31)

Dimensionless absorbed energy rate $\pi_2 = \frac{L^2 \dot{m}_c}{\mu_v} \cong \frac{L \dot{Q}^t}{\mu_v h_{fg}}$ (32)

Modified Prandtl number is the ratio of kinetic viscosity of the steam and thermal diffusivity of the wet paper, which indicates the influence of heat conduction on the heat transfer in the wet paper. Modified Schmidt number represents the effects of capillary flow on the water movement. Phase change number denotes the ratio of specific heat and latent heat, and Darcy number indicates the flow resistance of the porous media. Dimensionless number π_1 and π_2 are unique; π_1 is the dimensionless suction pressure representing the dimensionless driving force of pressure-driven flow, and π_2 is the dimensionless absorbed energy rate. Here a product of Da and π_1 becomes useful dimensionless number, which characterizes mass flow rate of steam. We define the dimensionless number Ω and π'_2 as follows.

Dimensionless mass flow rate of steam $\Omega = Da \cdot \pi_1$ (33)

Dimensionless average absorbed energy rate $\pi'_2 = \frac{\bar{Q}}{\mu_v h_{fg}}$ (34)

Where \bar{Q} is the average absorbed energy rate until absorbed energy Q reaches the 80% of the maximum absorbed energy. Maximum absorbed energy is equal to the heat requirement to raise the sample temperature to the steady state value.

5. Discussion

Fig. 8 shows dimensionless absorbed energy rate π_2 at $\Omega = 3.16$ and 6.0. As mentioned earlier, influence of capillary conductivity on the absorbed energy rate is parametrically studied. This is tantamount to vary the value of modified Schmidt number Sc' . The lines a and b in the Fig. 8 are the calculation results for the fine paper. We use a value four times the value of the capillary conductivity by Han and Ulmanen for a , and the value by Han and Ulmanen is applied for b . The lines c and d are the calculation results for the newsprint, where the value of Han and Ulmanen for c and one-fourth value is applied for d . Increment in the capillary conductivity reduces modified Schmidt number Sc' . For the relative permeability, we use $n=3$ for the newsprint and $n=2$ for the fine

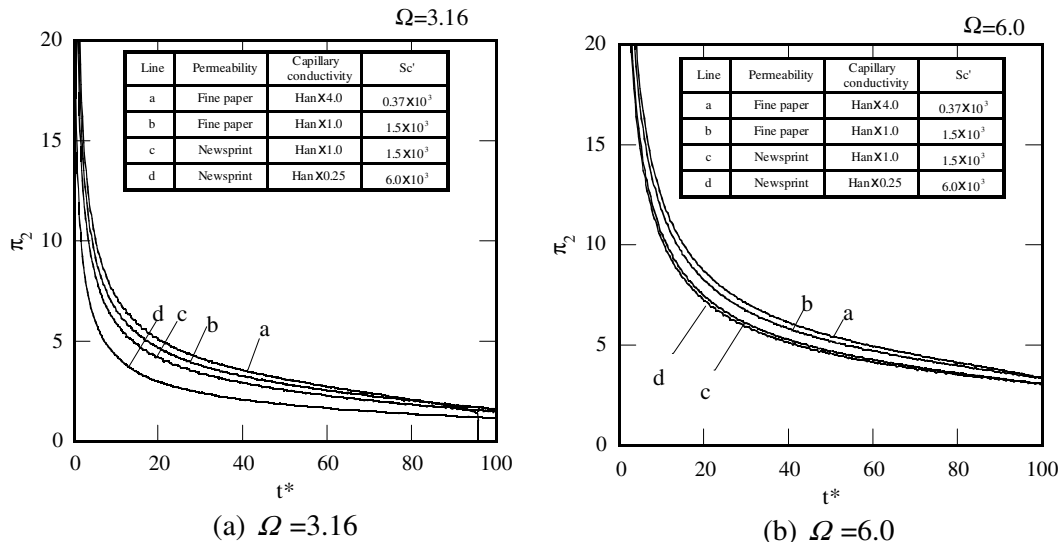


Fig. 8. Absorbed energy rate π_2 .

paper. At the same modified Schmidt number Sc' and flow rate Ω , the absorbed energy rate π_2 of newsprint is smaller than the fine paper. Newsprint has a larger n than the fine paper. Therefore, the permeability of the newsprint is easily affected by the increasing moisture content, which prevents the steam flow into the wet paper. Fig. 9 shows moisture and pressure distributions in the thickness direction at the $\Omega = 3.16$ and 6.0. An example of low ab-

sorbed energy rate, Fig. 9(a) and (c) show the calculation results of the newsprint ($n = 3$) with one-fourth capillary conductivity value ($Sc' = 6.0 \times 10^3$). Also, an example of the high absorbed energy rate, calculation results for the fine paper ($n = 2$) with the quadric capillary conductivity value ($Sc' = 0.37 \times 10^3$) are shown in Fig. 9(b) and (d). The moisture content increases with heating time due to the internal steam condensation and the spreading of the condensa-

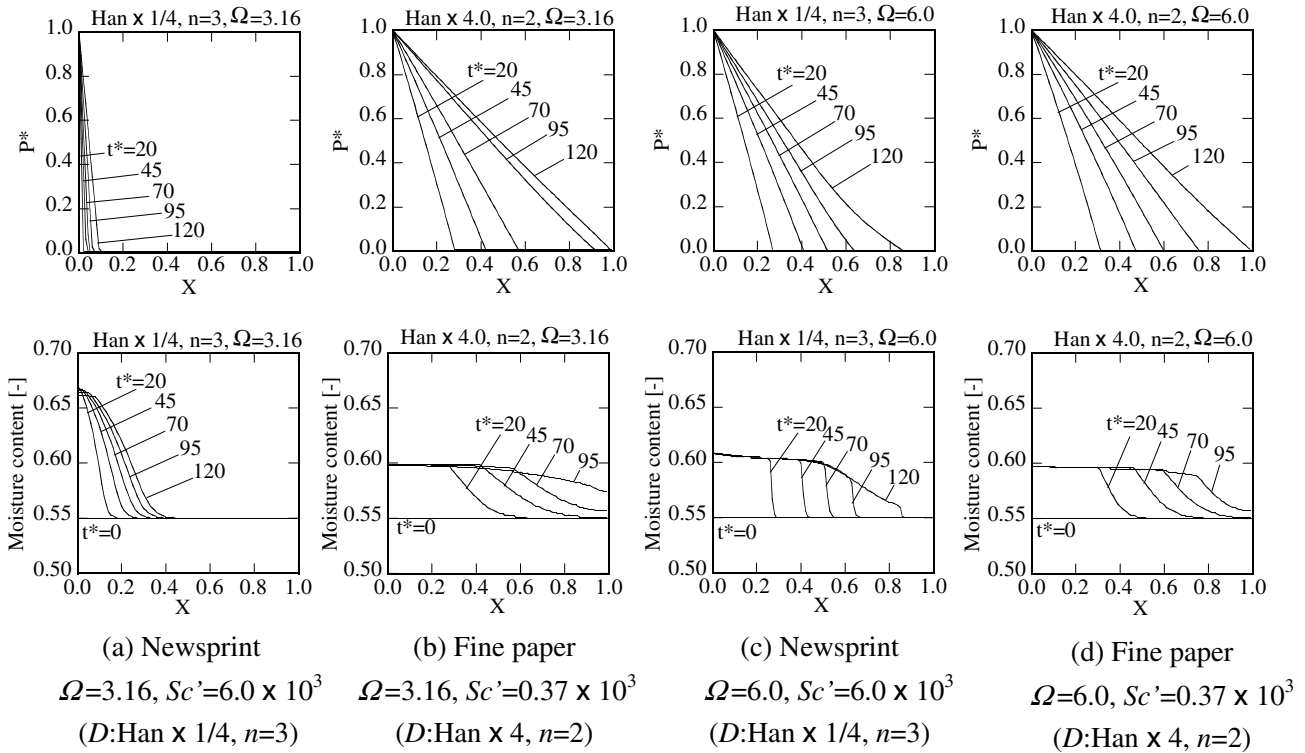


Fig. 9. Pressure and moisture distribution.

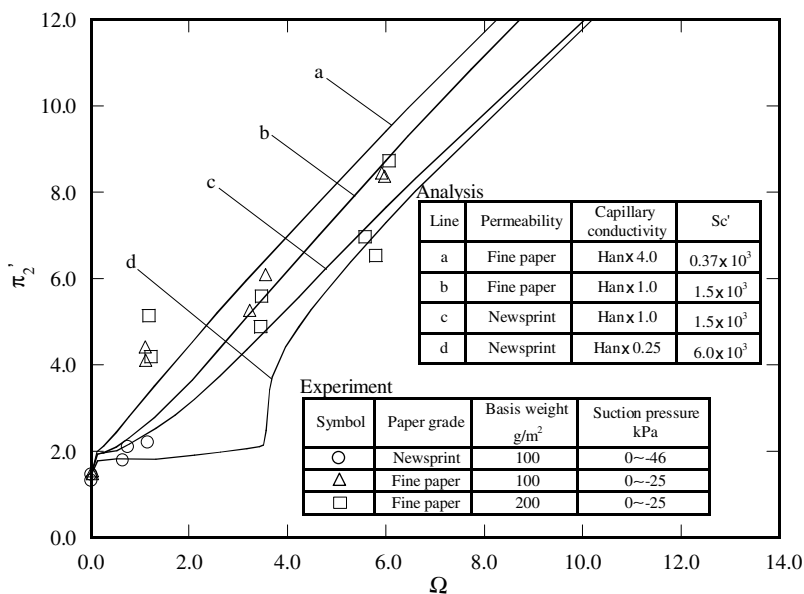


Fig. 10. Relation between Ω and π_2 .

tion region reduce the pressure gradient. Increasing of the moisture content and decreasing of pressure gradient reduce the mass flow rate of steam and energy absorption rate. As shown in the Fig. 9(a) and (c), in the case of high Sc' , the moisture content at the surface region becomes relatively high. So, reduction of the permeability is large in comparison with the low Sc' case, and mass flow rate of steam and absorbed energy rate become relative low. For the high Sc' case, the moisture content at the surface region increases with decreasing Ω (Fig. 9(a)). When Ω is small, the mass flow rate of steam is also small, and the steam is consumed by the internal steam condensation near the surface region and other region is mainly heated by the heat conduction. Therefore, moisture content at the surface region rises drastically. For the small Ω with high Sc' , an increase in the moisture content at the surface region mainly decreases the absorbed energy rate. In the case of low Sc' (Fig. 9(b) and (d)), the water generated by the internal steam condensation flows to the downstream rapidly, and the moisture content at the surface region is maintained at relatively low level, even if Ω is small (Fig. 9(b)). In this case, most of the region is directly heated by the internal steam condensation and only the bottom region is heated by the heat conduction. For the case of Fig. 9(c) where Ω is large enough, the moisture content at the surface is relative low and most of region is heated by the internal steam condensation even in the high Sc' condition. When Ω is sufficiently large, the steam velocity in the wet paper is faster than the thermal diffusion velocity. Thus, the internal steam condensation can be used to heat both near-surface region and inner region.

The non-dimensional relation between the steam flow rate Ω and the average absorbed energy rate π'_2 is shown in Fig. 10. In the figure, analytical results *a* and *b* are for the fine paper, and *c* and *d* are for the newsprint. Calculation conditions are the same as Fig. 8. Experimental results are also included in the figure and we can see all of the data for newsprint are plotted in the smaller Ω range. Since the lower permeability of the newsprint is not so effective for the suction flow, only heat conduction can be used to heat up the wet paper. On the other hand, the experimental energy absorbed in the fine paper increases in proportion to the steam flow rate regardless of the basis weight of paper. Since the theoretical results correspond with these experimental data very well, it is considered that the dimensionless number Ω and π'_2 are useful to estimate the effect of suction pressure on the energy absorption. From the theoretical line *a* for the fine paper with low Sc' , we can see that π'_2 increases with Ω and can understand the paper is directly heated by the internal steam condensation. In the case of high Sc' (line *d*), there is a region of constant absorption energy without depending the steam flow rate. It is clear that the wet paper is mainly heated by the heat conduction in this region. Even in the high Sc' (line *d*), however, the heat transfer in the wet paper changes from the heat conduction to the internal steam condensation if Ω is larger than a certain value.

6. Conclusion

We studied heat and mass transfer of the wet paper in the steam heating process experimentally and analytically. Two unique dimensionless numbers, Ω and π'_2 are derived from the basic equations to express the relation between the mass flow rate of steam in the wet paper and the average absorbed energy. Experimental and numerical results are summarized by using these dimensionless numbers and the following conclusions are obtained.

- (1) Suction pressure enhances energy absorption into the wet paper and its effects are marked in the high-permeability paper.
- (2) In the case of small Ω with high Sc' , the absorbed energy rate is decreased with increasing of the moisture content at the surface region, and heat transfer in the wet paper is dominated by the heat conduction.
- (3) In the case of large Ω , decreasing of pressure gradient reduces the absorbed energy rate, and the wet paper is mainly heated by the internal steam condensation.

Acknowledgement

The authors wish to thanks to Mr. H. Hirano and Mr. H. Nagai for their contribution to this study.

References

- [1] K. Cutshall, D. Hudspeth, Hot pressing, Tappi Seminar Discuss. (1988) 239–250.
- [2] T. Patterson, J. Iwamasa, Review of Web Heating and Wet Pressing Literature, 1999 TAPPI Papermakers Conference, Atlanta, GA, 1999, pp. 1255–1278.
- [3] T. Patterson, M.A. Strand, D.I. Orloff, An apparatus for the evaluation of web-heating technologies – development, capabilities, preliminary results, and potential uses, TAPPI J. 79 (3) (1996) 269–278.
- [4] T. Patterson, J. Iwamasa, Steambox Comparator Experiments: Apparatus Validation and Investigation of Steambox Performance, 1999 TAPPI Engineering Conference, Anaheim, CA, 1999, pp. 621–635.
- [5] T. Patterson, An investigation of factors affecting stambox heating effectiveness, TAPPI J. 1 (7) (2002) 8–12.
- [6] C.J. Nederveen, J.G. Finken, Thermal conductivity measurement on wet paper samples at high temperatures, Dry. Technol. 10 (1) (1992) 189–198.
- [7] Y. Hoshi et al., Prediction of temperature and moisture content profiles of paper in drying process, Trans. Jpn. Soc. Eng. B 64 (625) (1998) 281–288 (in Japanese).
- [8] T. Kadoya et al., Science of Papermaking, chugai sangyo chosakai, Tokyo, Japan, 1982, pp. 94.
- [9] T. Kawamizu et al., Effects of suction pressure on heat and mass transfer during steam heating of wet paper, Dry. Technol. 25 (2007) 1045–1052.
- [10] M. Kaviany, Principles of Heat Transfer in Porous Media, Second ed., Springer, New York, 1995, pp. 480–496.
- [11] M. Karlsson, Paper Making Part2, Drying, Fapet Oy, Finland, 2000, pp. 54–83.
- [12] P. Chen, D.C.T. PEI, A mathematical model of drying processes, Int. J. Mass Transfer 32 (2) (1989) 297–310.
- [13] S.V. Patankar, Numerical Heat Transfer and Fluid Flow, McGraw-Hill, New York, 1980.